INTERFERENCES ON CIRS INTERFEROGRAMS AND SPECTRA

A User Guide

May 23rd 2005

Conor A. Nixon, Virgil G. Kunde (Univ. MD)
Ronald C. Carlson, Andrei Mamoutkine (SSAI)
Donald E. Jennings, John Brasunas, Michael Flasar (NASA GSFC)

TABLE OF CONTENTS

LIST OF FIGURES

LIST OF TABLES

ACRONYMS AND ABBREVIATIONS

AACS	Attitude and Articulation Control System.
BIU	Bus Interface Unit.
CCRCO	Cooler Cover Release Check-Out Test, May 27th 2000.
CDS	Command and Data Subsystem.
CEA	Central Electronics Assembly (CIRS).
CIRS	Composite Infrared Spectrometer.
DOY	Day Of Year.
FFT	Fast Fourier Transform.
FP	Focal Plane (1,3,4 on CIRS).
FSWCO2	Flight Software Check-Out #2, June 2000 (?).
ICO1	Instrument Check-Out Test #1, January 1999.
IFM	Interferogram.
MAPS	Magnetosphere And Particles Science – generic term for six instruments on Cassini: MIMI, RPWS, CAPS, CDA, MAG, and INMS.
MIMI	Magnetospheric IMaging Instrument
OOL	Out Of Lock (see PLL).
PLL	Phase Locked Loop (CIRS).
RPM	Revolutions Per Minute.
RTI	Real Time Interrupt.
RWA	Reaction Wheel Assembly.

1.0 Introduction

This document is intended to both summarize the origins of, and methods of removing, the various types of interferences seen on CIRS interferograms (IFMs). Both 'ubiquitous' and 'transient' types are discussed: these categories roughly correspond to 'electronic' and 'mechanical' disturbances respectively. Enough detail should be supplied herein both for the casual user, who merely wishes to understand and avoid artifacts on the spectrum, and for the more sophisticated user who may wish to undertake a calibration of the spectra from raw interferogram data.

Please send comments to: conor.nixon@gsfc.nasa.gov

2.0 Characterization of Interferences

2.1 Ubiquitious Interferences

2.1.1 BIU Spikes

During the first Instrument Check-Out test (ICO1) performed after launch, it was noticed that a pattern of large spikes at quasi-regular intervals was evident on the FP1 interferograms. These occurred with intervals of 11, 11, 10, 11, 11, 10 (repeated) RTIs and was soon determined to originate in the Bus Interface Unit (BIU). Querying of the BIU by the spacecraft CDS at a frequency of 0.75 Hz to transfer cached data, led to interferences at 1.333 second intervals, which was subsequently discretized to the nearest 1/8 of a second (1 RTI). See Appendix A for a fuller description. From the Cooler Cover Release Checkout onwards, the CDS interrupt rate was changed to 0.5 Hz.[1]

This made matters much simpler, because the repeat cycle became 1 interrupt every 2 seconds, or every 16 RTIs, insteadof the more complex 11, 11, 10 RTI pattern. On FP1, this interrupt rate predicts that we should see spikes with a period of 16 x 7.404 = 118.464 samples. In fact, on the IFM we hence see spikes at intervals of 118, 119, 118, 119 etc, approximately, due to the discretization. The new spike pattern in samples is:

Equation 1: formula for sample number of BIU spikes.

$$s_n = INT(S_0 + (7.404 \times 16n)), \quad n = 1,2,\ldots$$

Where S_0 is the offset in samples of the first spike from start of scan.

If the IFM scan length is an exact multiple of P RTIs (with P currently =16) then clearly the interference will occur in about the same place on successive scans. In general,

[1] Apparently because CIRS was not filling the packets completely at the higher rate.

however the BIU spikes will not line up on successive scans. The number N of IFMs required to complete the cycle is given by Equation 2:

Equation 2: formula for repeat period of BIU spikes.

$$N = \frac{L.C.M.(R,P)}{R}, \qquad R = \mathrm{mod}\, P$$

where R is the 'remainder' of RTIs at the end of a scan, L is the length of a scan in RTIs, P is the period of the interference pattern in RTIs, and N is number of scans for the interference pattern to repeat. L.C.M. indicates taking the Lowest (Least) Common Multiple.

For example, at CCRCO a scan of 404 RTIs had a repeat period of 4 IFMs (Figure 1) while a scan of length 224 RTIs repeated the interference on every scan (Figure 2). In short, any scan which has a length in seconds which is an even whole number, will have the same spikes in the same place on every scan.

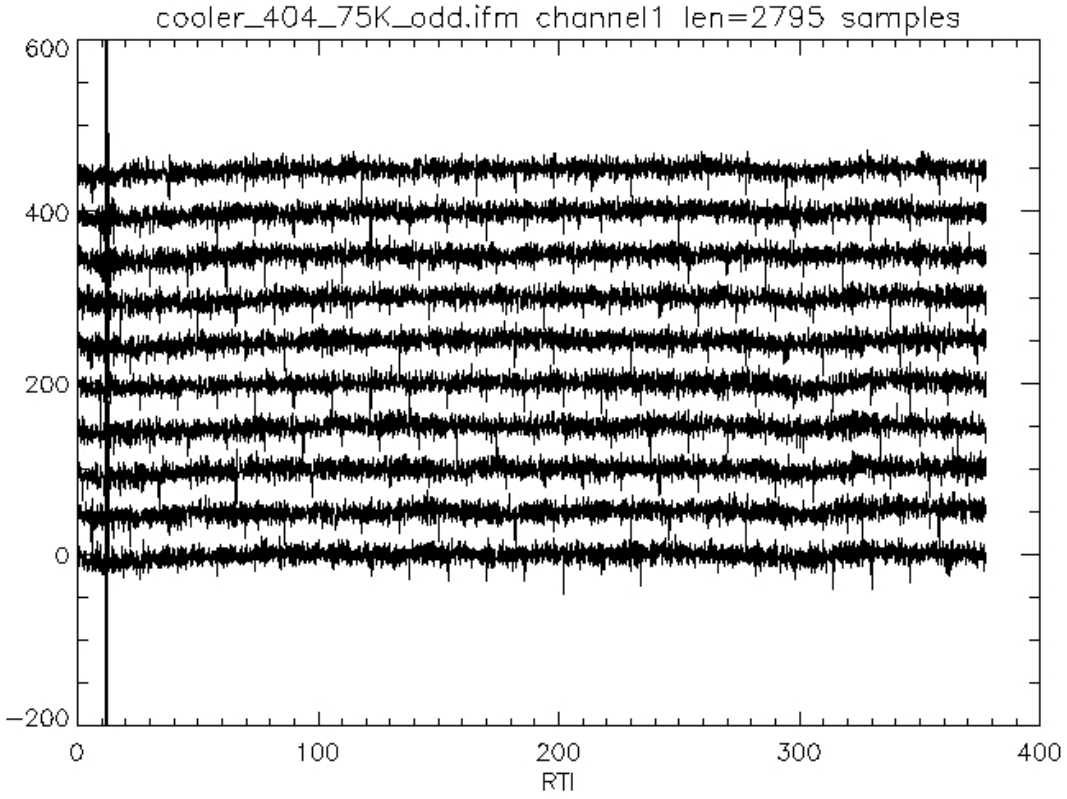

Figure 1: sequence of ten 404 RTI, FP1 scans from the (CCRCO) test data. The large BIU interference spikes are repeated every fourth scan. The scan numbers are 26 (bottom plot) to 35 (top plot), and have been deliberately offset by increments of 50 counts in the y-direction.

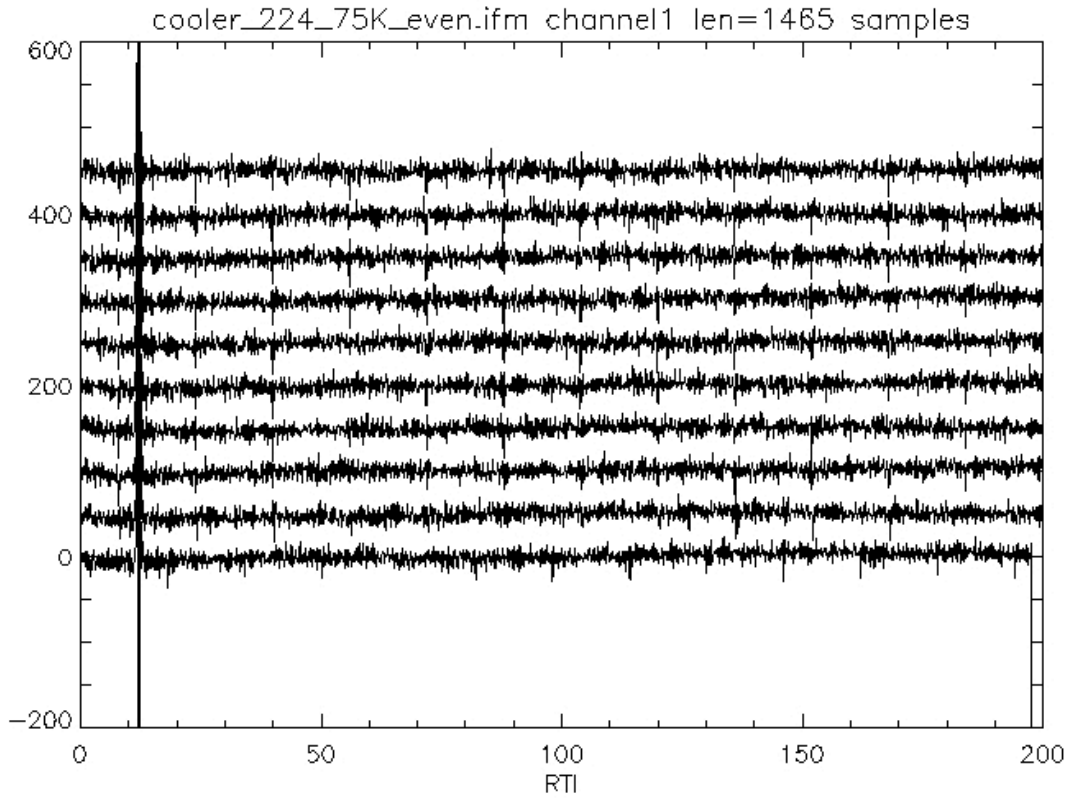

Figure 2: FP1 scans from Cooler Release Checkout. T_{FPA}=75 K, 224 RTI. The scan numbers are 26 (bottom plot) to 35 (top plot), and have been deliberately offset by increments of 50 counts in the y-direction.

2.1.2 8-Hz RTI Clock Spikes

These spikes are small and are buried in the noise on the IFMs. However, they appear clearly on the spectrum at 8 Hz, 16 Hz and 24 Hz on FP1, and also 32 Hz and 40 Hz on FP3 spectra. The 8 Hz prime frequency is due to the RTI count. The 8 Hz and 16 Hz peaks are clearly visible on Figure 3.

2.1.3 Sine Wave

This interference appears as a sine ripple on the FP1 IFMs, and as a large spike on the spectra. Its frequency changes over time (moving peak on Figure 3) and has been seen in the range ~1-18 Hz (at least). In general, the frequency seems to decrease over time when the instrument is fully powered on in science mode. The source is unknown, but suspected to have a thermal source. In addition, when the principle frequency of this peak f_0 is above 8 Hz, a lower, weaker beat frequency f_1 is seen at $f_0 - 8$ Hz. This is more clearly seen in co-added spectra. When $f_0 < 8$ Hz, the beat is no longer seen. There is also an even weaker beat at $f_0 + 8$ Hz.

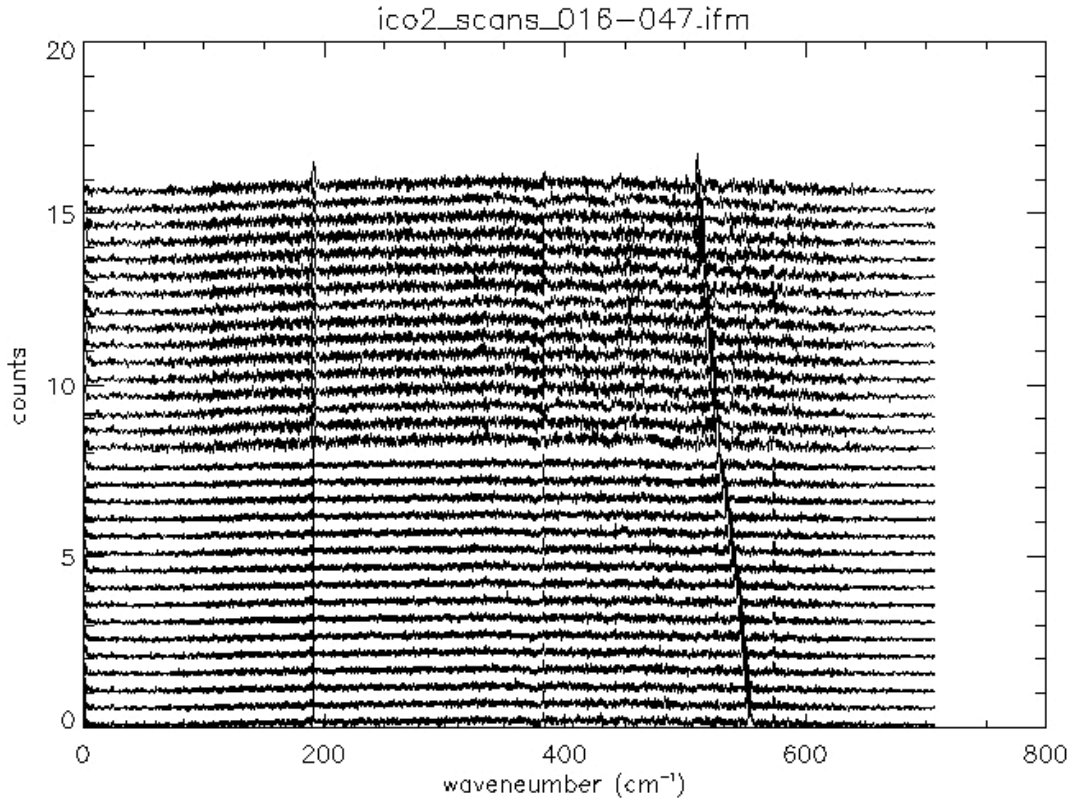

Figure 3: Spectra produced by raw FFT of FP1 scans from Instrument Checkout #2. The scan numbers are 16 (bottom plot) to 47 (top plot), and have been deliberately offset by increments of 0.5 counts in the y-direction. Scans 16-31 are for odd detectors, 224 RTI. Scans 32-47 are for even detectors, 112 RTI.

The temperature dependence of this interference has been studied. Figure 4 below shows a plot of the sine wave frequency versus the electronics board temperature (CEA) for three data-taking periods in the cruise phase of the mission: Instrument Check-Out Test #2 (ICO2), Cooler Cover Release Testing, and Jupiter Encounter.

The results show that the sine wave frequency does decrease linearly as the CEA temperature increases. However, the gradient was substantially steeper at the time of the cooler cover release check out than at the other two periods. The exact reason for this is not known, but it appears that the sine wave interference is not directly caused by the electronics board heating. Instead, the electronics board temperature serves as a partial indicator of the problem. Suspicion has been thrown onto the temperature/power of the optics assembly.

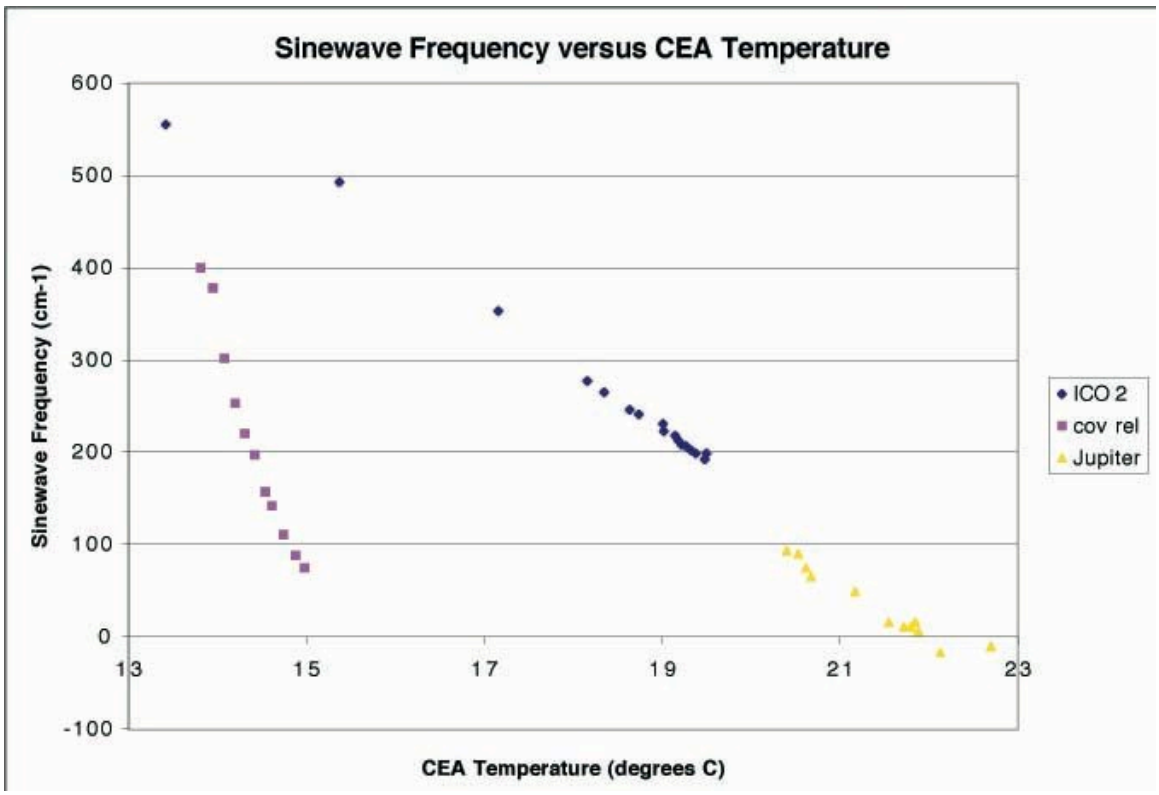

Figure 4: plot of sine wave frequency versus CIRS central electronics assembly temperature.

2.2 Transient Noise Sources

The transient noise sources referred to here are mechanical disturbances, which cause the mirror scan mechanism to lose lock and/or suffer jitter or other speed variations. Two sources have been identified: (i) the spacecraft reaction wheels, and (ii) actuator of the LEMMS particle detector on the MIMI instrument. These will be considered in turn.

2.2.1 Reaction Wheels

Around the start of 2005, it was noticed that CIRS was returning a significant number of IFMs with a greater than normal number of samples. Further investigation discovered that in most cases, the Phase Lock Loop, which regulates scan mirror velocity was also out of lock (OOL). The problem seemed to be especially bad during DSCAL sequences: deep space observations during spacecraft to Earth data downlink. Many of these sequences were taken while the spacecraft was rolling around the –Z axis to enable MAPS (Magnetosphere and Particles Science) instruments to collect data.

Figure 5 below shows an example of a DSCAL sequence on DOY 26. The blue dots show the number of samples in an IFM, compared to the PLL parameter (green). When

the PLL is 1 (OOL), abnormally high numbers of samples are recorded. The horizontal dashed line near 1500 shows the normal sample number level.

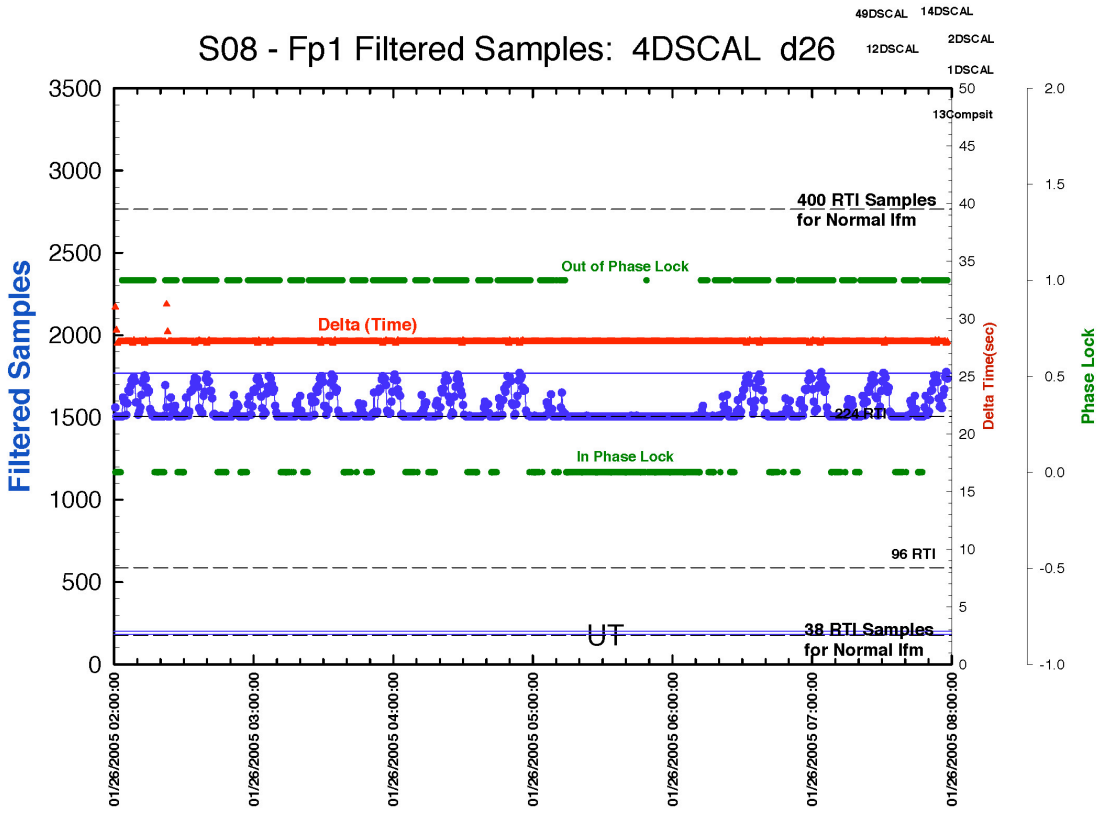

Figure 5: number of FP1 filtered samples (blue) compared to PLL parameter for 2005 DOY 26. The number of samples regularly exceeds nominal when the PLL=1 (Out Of Lock).

Figure 5 may be compared to Figure 6 (below) which shows the opposite case during a DOY 27 FMONITOR rings observation, where the PLL was predominantly zero, and the number of samples did not significantly deviate from the normal level.

The loss of phase lock has been found to be related to the reaction wheel assembly (RWA) movements, but in a complex manner. When the wheels are in motion, the loss of phase lock is more often observed, although there are exceptions. In general, the higher the wheel speed, the more likely that a disturbance to CIRS is noticed. Also, it appears that there may be a mechanical resonance effect when the reaction wheels spin at a speed of 1250-1300 RPM, increasingly the likelihood of disruption. If this speed can be avoided in future, it may be possible to minimize the disturbance.

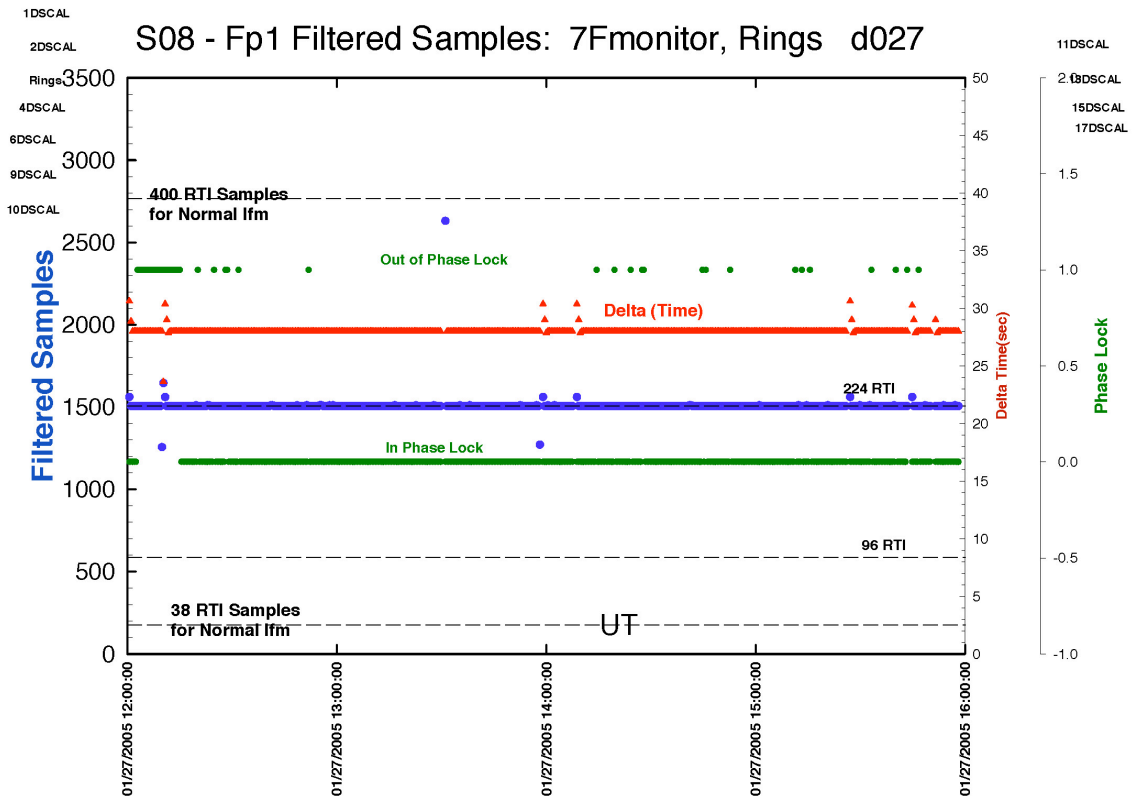

Figure 6: number of FP1 filtered samples (blue) compared to PLL parameter (green), for 2005 DOY 027.

2.2.2 MIMI LEMMS

A second type of mechanical disturbance, which also caused loss of phase lock, was traced to the LEMMS detector on the MIMI instrument. Figure 7 shows an example of this disturbance during a Saturn observation, although Titan observations were also affected. The effect became most noticeable in January-February 2005, and affected target-specific interferograms. Subsequently, the MIMI LEMMS actuator was shut down in mid-February and there has been no problem from this cause since then.

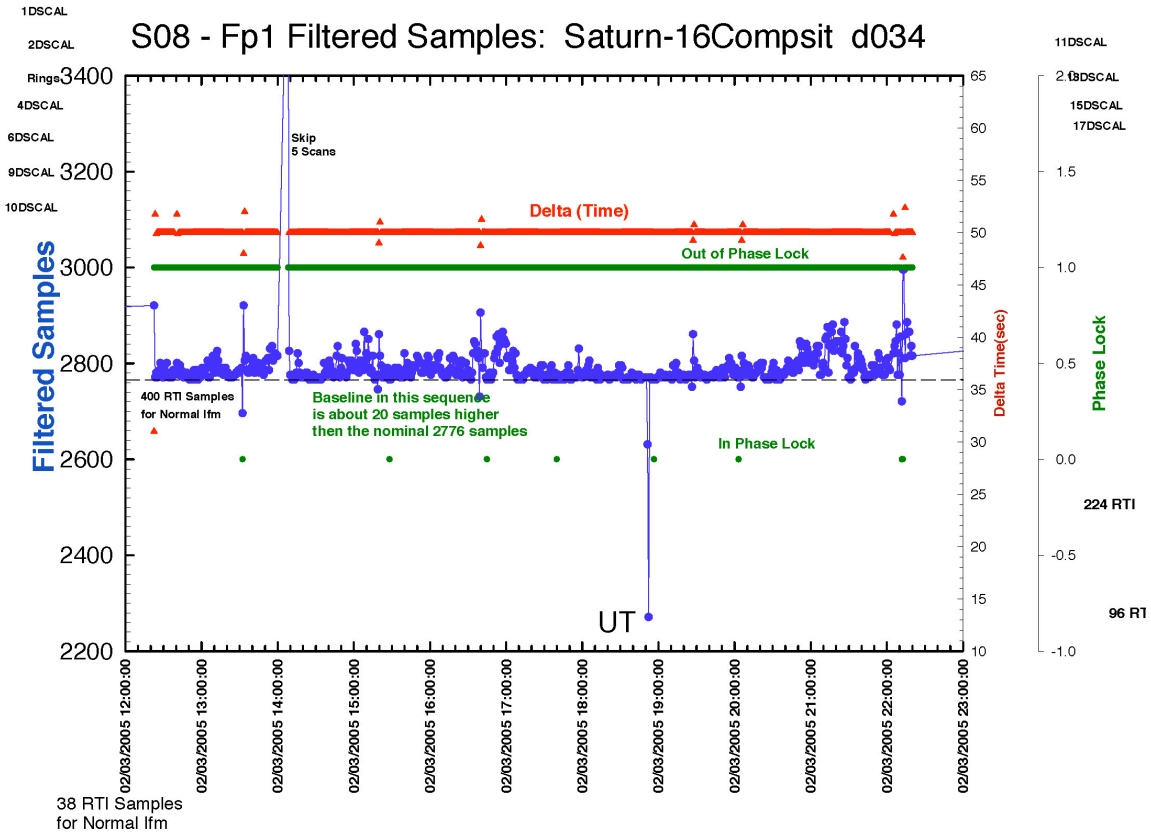

Figure 7: interference from the MIMI LEMMS detector during a Saturn CompSit observation.

3.0 Removal of Interference

3.1 Removal of BIU Spikes on single IFM

The BIU spikes have been observed to occur at 0.75 Hz (ICO1) and 0.5 Hz (subsequently). The discussion here is confined to the 0.5 Hz spikes, but the methodology would be very similar for 0.75 Hz spikes.

The spike frequency of 0.5 Hz corresponds to a spike interval of 2s=16 RTI. For FP1, the sample rate after decimation is 59.232 filtered samples/second, hence the spikes are predicted to occur every 118.46 samples on the IFM, which is the observed period.

There are two main approaches to removing the interference on a single IFM:

1. **Interferogram (spatial) domain.** Subtract a 'comb' of spikes adjusted to be at the right interval and amplitude to correspond closely to the interference spikes.

Advantages: the relative positions of the spikes are exactly known. Disadvantages: the absolute spike positions vary, as do the amplitudes.

2. **Frequency (spectral) domain.** Remove the spikes at discrete frequencies, remembering that harmonics of the 0.5 Hz are seen. Advantages: absolute positions of the interference known. Disadvantages: amplitudes not known; also may be confusion with spectral lines.

At this point, removing the BIU interference in the spectral domain (method 2) has not been seriously attempted. One reason for this is that a planetary spectrum may well show features of interest (spectral lines) at similar positions to the interference spikes, making determination of the interference amplitude problematic.

In the IFM domain (method 1), we have the advantage of knowing that large, regular spikes away from the ZPD are certainly interference; there is much less confusion than in the spectral domain.

One of the key problems when working in the IFM domain is to determine the absolute offset position of the spike pattern (S_0). There are several possibilities for doing this:

1. Determine manually by inspection.
2. Automatic determination by cross-correlation of a sample comb with the data IFM.
3. Predicted based on some other information.

Each of these alternatives is examined in turn.

3.1.1 Manual method

The first suggestion is that a 'comb' pattern of spikes may be created as an interference template, and subtracted from the data spectrum to remove the interference.

In detail, a comb or shah function is created which has the appropriate frequency interval, determined by the BIU frequency (0.5 or 0.75 Hz). Although the spacing of the spikes is predictable, the absolute offset S_0 must be determined by manual inspection of the data spectrum. However, in cases where the RTI length of the scan plus fly-back is an exact multiple of the interference interval in RTI, e.g. 224 and 16, the offset will be repeated on all IFMs after the first. Hence, the offset need only be determined once.

Once the offset has been determined, the spike pattern is scaled to match the mean size of the interference spikes on the data, again determined by eye, and subtracted to leave an interference-free (or greatly reduced) IFM.

This method produces good results. The main drawbacks are that the offset of the spikes and the height of the comb pattern must be determined manually. In addition, it is important to check each spectrum to make sure that the spike pattern has not shifted, as is

occasionally observed. This means that the method is impracticably slow for large numbers of spectra.

3.1.2 Cross-correlation method

In fact the comb-subtraction approach may be automated by adding automatic determination of the comb offset and amplitude.

The frequency of the spikes is assumed as before but not the absolute positions. A comb is created of the appropriate spacing, which is then used as a template. The cross-correlation function of the comb with the data is then computed to find the absolute offset. Not all the data is used. The short two-sided portion close to ZPD is excluded, because otherwise the highest correlation would always occur when the spikes lined up with the IFM peak value.

Once the offset has been calculated, the spike pattern is calculated for the entire (short plus long side) IFM. The magnitude of the spike pattern is taken to be the mean value of the data at the positions of the spikes. Finally, the scaled comb is subtracted from the data.

In the current implementation, predicted spike locations are also double-checked against spikes detected by a statistical technique. Figure 8 demonstrates the process graphically. This method gives comparable results to the manual comb method, and is preferable due to speed.

The main problem with this method is common to all methods which assume a spike frequency and use a fixed interval: namely that the spike interval is not observed to be entirely regular. Spikes can occur one or two samples ‘late' or ‘early', and may also spread over two sample points rather than one. This may be due to the discretization of the RTI interval (7.404 samples) into whole numbers of samples, and needs to be examined closely.

In these cases, the subtraction of the comb from the wrong location will not only fail to remove the spike, but will introduce an additional one in the wrong direction. The issue to be resolved is: is it still better to subtract the comb than to leave the data with the interference? The answer appears to be that the final spectrum is improved.

Subsequent analysis of the spikes at high S/N on FP1 has shown the spike pattern is not a simple array of delta functions, as originally conceived. Instead, it is a complex ripple having peaks at the proscribed interval. Further refinements to the pipeline code for data processing should enable the ‘empirical comb’ to be subtracted, rather than the ‘theoretical comb’.

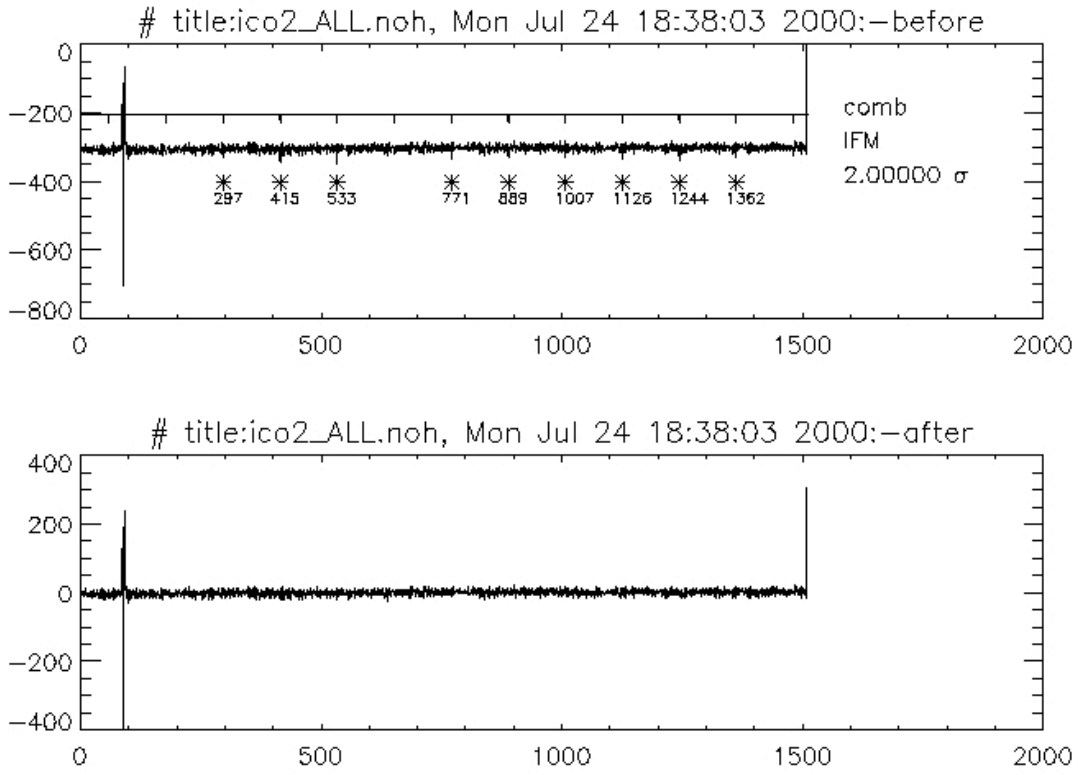

Figure 8: The process of subtracting a predicted spike 'comb' from the IFM. The upper IFM is before subtraction, the lower after comb subtraction.

3.1.3 Spike prediction based on start RTI count

It has been suggested that the start RTI value of each scan may be used to predict the offset of the first spike in samples. This proposal needs to be examined carefully.

Let us say for example that the BIU interrupt always occurs on RTI count 0. In fact, it will occur on alternate RTI=0, because the period of the BIU interrupt is 2 s, or 16 RTI, which is two full cycles. Therefore, if the scan actually starts on RTI=4, the first interference spike would be predicted to occur either 4 RTIs later, at sample 29.616 (29 or 30), or 12 RTIs later, at sample 88.848 (89 or 90). This two-fold degeneracy is the first but not the most serious problem with the spike prediction.

We can re-arrange equation Equation 1, splitting the term S_0 into two separate constants:

Equation 3:

$$s_n = (7.404 \times ((n \times 16) + S_1)) + S_2 \qquad n = 1,2,\ldots$$

where S_1 is the offset in RTIs of the first spike (either 4 or 8 in the above example), and S_2 is the offset of the BIU interrupt within each RTI count (0 to +7.404 samples).

The more serious problem is that, even if we know S_1 from the start RTI of the scan, we still have no idea about S_2 except empirically, through looking at the data. This still gives us large uncertainty in the spike positions.

Consider Figure 2 which shows ten consecutive FP1 scans from the cooler cover release checkout. The spike locations have been listed on Table 1. Now let us examine whether the start RTI really does predict the spike occurrences.

Table 1: sample positions of BIU interference spikes in FP1 interferograms, from the cooler cover release checkout test.

Scan Number	Start RTI	1	2	3	4	5	6	7	8	9	10	11	12	13
26	0	16	134	253	371	490	608	726	845	963	1082	1200	1319	1437
27	2	61	180	298	417	535	-	-	-	1009	1127	1246	1483	-
28	3	59	178	296	-	534	652	770	888	1007	1125	1244	1362	-
29	3	59	177	296	414	533	651	-	888	1006	1125	-	1362	1480
30	3	58	177	295	-	532	651	769	888	1007	1125	1243	1362	1480

The first spike of scan 26 starts at sample 16, which is approximately two RTIs after the scan start. Hence, this would indicate that the RTI of the inference is on RTI count 2. In scan 27, the first spike arrives at sample 61, or approximately 8 RTIs plus 2 samples after the scan start. This again indicates that the BIU is on alternate RTI=2. In scan 28, and subsequent scans, the first spike arrives at sample 59, exactly 8 RTIs after the scan start, which in these scans occurs at RTI 3. This indicates the BIU is at RTI 3.

On later scans (36-45), the start RTI varies between 2 and 3, while the interference spikes stay at roughly the same sample positions, but waver by a few sample points (Table 2). There is some indication that when the start RTI is two, the spikes occur at 2-3 sample points later than usual, indicating that the BIU may occur on the change point from RTI 2 to RTI 3.

Table 2: position of BIU interference spikes in FP1 interferograms from the CCRCO test.

Scan Number	Start RTI	1	2	3	4	5	6	7	8	9	10	11	12	13
36	3	59	177	295	414	532	651	769	-	1006	1124	-	1361	1480
37	2	61	179	298	-	534	653	772	889	1008	1127	1243	1363	1482
38	3	59	177	295	414	532	651	770	888	-	1125	1243	1363	1480
39	3	61	177	295	414	532	653	769	887	1006	1124	1243	1363	1480
40	3	59	177	296	414	533	651	770	888	1107	1125	1243	1362	1480

In summary, predicting the absolute position of the spikes from the start RTI does not seem to be feasible. Knowing the scan start to within one RTI is not enough, we also need to know to within one sample position where in the RTI we are, so that we can predict exactly when the changes in RTI occur.

3.2 Removal of BIU spikes on multiple IFMs

Several other methods become feasible for eliminating or reducing the BIU spike amplitudes, if multiple target spectra can be calibrated together. However, both these methods reply on the data being taken at certain RTI lengths, which are not whole multiples of 16 (2s), to ensure that the spikes do not remain in the same place on consecutive IFMs,

1. **Pairing and windowing.** In this method, pairs of IFMs are considered together. The spike pattern must have a different offset in both IFMs, preferably being a full eight RTIs (1s) apart. The spikes are then cut out of both IFMs, and the remaining data is weighted and co-added to produce a full IFM.
2. **Cycling to 8 Hz.** In this method, a scan length of 16n+1 RTIs is used to cycle the BIU spike pattern between the 16 possible offset positions. If these 16 individual spectra are then co-added, the 0.5 Hz pattern becomes an 8 Hz spike pattern, and overlays the existing 8 Hz spikes. If deep space and shutter are processed in the same way as target scans, then the entire pattern will cancel during calibration, for FP3 and FP4.

These two methods are now considered in more detail.

3.2.1 Pairing and windowing

For a spike pattern at 0.5 Hz (2s intervals) a large spike occurs every 16 RTIs. Therefore there are 16 possible offset positions of the spike pattern on the IFM from start of forward scanning motion. This is because a scan always begins exactly on an RTI pulse from the spacecraft. However, note:

1. The exact offset is affected by a number of factors, including the length of the mirror fly-back time from the end of the previous scan. So, when the RTI length of the IFM changes, the offset will change as well.
2. Mirror speed variations may also affect the recorded position, even if the RTI length is unchanged.

Depending on the value of the ‘remainder’ RTIs when the scan length is divided modulo 16, the spike pattern may remain static or cycle through various offset values with a repeat cycle off up to 16 scans. For example, any RTI length which is an exact multiple of 16 will have the same offset on all scans. However, an RTI length of 16n+1 (n integer) will have a repeat cycle of 16.

From approximately 2000-2004 the CIRS team aimed to use scan lengths of 16n RTIs, for the reason that average deep space and shutter IFMs would have the same spike positions as single target IFMs. Hence, these should cancel out during calibration, at least for the mid-IR detectors,

The ‘pairing and windowing’ technique on the other hand suggests that a scan length of 16n+8 RTIs is used instead. In this way, the spike pattern on successive scans cycles through a repeat pattern of 2, alternating in an A-B-A-B etc manner. Now, the portions of the ‘A’ IFM which contain BIU interference spikes are spike-free on the ‘B’ IFMs, and vice versa. Hence, by combining information from a single ‘A’ and ‘B’ IFM, a complete spike-free IFM can be built up.

In practice, the technique applies the following steps:

1. Determine the offset of the spike pattern on the ‘A’ IFM.
2. Window-out, or mask the spikes regions on the ‘A’ IFM. For example, if the first spike is at sample 50, then a region 48-52 would likely be masked out. The exact size of the window may be varied, but several points on either side of the main peak should be sufficient to remove most of the spike power.
3. Similarly mask out the spike regions in IFM ‘B’.
4. Finally, the two IFMs are combined with appropriate weights. Data regions which are not masked on either IFM are added by arithmetic mean (co-add and divide by 2) whereas region which are windowed on one IFM but not the other are simply copied. I.e. they have a weighing of 1.

Note that this method assumes that the three other contributions to spectral power have well defined characteristics. In particular:

1. That the target information is constant between the ‘A’ and ‘B’ scans, so is better suited to integration-type observations than to spatial scanning.
2. That the random noise has a white-noise power spectrum.
3. That the 8 Hz spike pattern is the same on the ‘A’ and ‘B’ scans.

To date, this method has not been extensively put into practice although some tests have been made with promising outcomes. The main difficulty with this method is in the ground processing.

3.2.2 Cycling

The ‘cycling’ method uses a scan length of 16n+1 to cycle the 0.5 Hz spike pattern through all possible positions. Then, blocks of 16 or more scans can be coadded, which distributes and dilutes the power by a factor 16, and turns the 0.5 Hz pattern into an 8 Hz pattern. As an 8 Hz interference pattern already exists, the two become overlaid. During calibration therefore, the 8 Hz pattern on the shutter, target and space IFMs should cancel out and disappear.

In practice, it is not generally desired to have the target IFMs calibrated in blocks of 16, which could correspond to quarter-hour time blocks. For this reason, the full co-adding potential of this method has not been implemented into the regular pipeline processing.

However, this type of processing could be done in certain cases off-line, if the data had been collected with the appropriate scan length to allow this.

However, even when processed through the regular calibration procedure, the 16n+1 length IFMs appear to show better noise characteristics than 16n length IFMs, when individual calibrated spectra are co-added. Why? The reason is that the 0.5 Hz noise pattern in the spectral domain has both amplitude and phase. When the spike pattern on the IFM is constant, the amplitude and phase on the spectra are also constant. However, when the spike pattern offset on the IFMs is shifted, the phase of the spikes in the target spectra is changed. This allows the overall amplitude to be reduced by co-adding spectra at different spike phase.

For this reason, a decision was taken in late 2004-early 2005 to change all standard IFM RTI lengths to a 16n+1 standard rather than 16n. Hence, 96 RTI became 97 RTI. 400 RTI became 401 RTI etc.

3.3 RTI spikes

Because these spikes occur on every RTI, and because the instrument scanning must always begin on an RTI, these spikes will always be synchronised on scans which have the same number of RTIs. The exception is the first scan of a block after the RTI length has just been changed, due to the anomalous fly-back time. Also, blocks at different RTIs will differ in offset for the same reason.

At constant RTI, these spikes are expected to cancel out (at least reduce in size greatly) when IFMs are subtracted during the calibration procedure (see appendix C). This process should work better when averaged IFMs rather than single IFMs are used, because fluctuations in the spike amplitudes will tend to be smoothed out. This procedure should remove the 8 Hz fundamental spike on the spectra and all overtones to a good approximation.

3.4 Interferogram Sine Wave

This interference is hard to account for in an automatic procedure, because its amplitude and frequency may both wander. Until a better model of this interference is determined, it may have to be dealt with manually on a scan-by-scan basis.

3.5 RWA Disturbance

A work-around is currently being devised which involves biasing the wheels to frequencies away from the resonances at 1300 rpm, whilst still avoiding too-high rates (shortens wheel life times) and too-low rates (wheel lubricant is not evenly distributed and sticking of wheels can occur).

3.6 MIMI LEMMS Disturbance

The LEMMS actuator was deactivated on 2005-050, and is not expected to cause further problems for CIRS.

4.0 Implications and Recommendations

Several key points can now be made which have implications for the way the data is generated and handled:

1. **The first scan after the scan length has been changed set is unique.** Consider that 10 scans are taken at 100 RTI followed by 10 scans at 200 RTI. The first IFM of the 200 RTI set will be longer than the next nine. The reason for this is that each 'scan' begins with the fly-back of the mirror from the end of the previous scan. Hence, for the first scan at 200 RTI, the mirror will only be returning from the end of the previous 100 RTI scan. However, subsequent 200 RTI scans will be subject to the longer fly-back. As the total time for fly-back + forward scanning is commanded, not the forward scanning time itself, the amount of time remaining for data taking will be greater in the first 200 RTI scan. In other cases, the first scan of a same-length set may have a shorter IFM if the preceding set was of longer time. In general, it may be desirable to throw out the first scan of every set to achieve homogeneity.
2. Assuming that the BIU interference remains at a frequency of 0.5 Hz, then any scans commanded to an EVEN number of seconds (multiple of 16 RTI) should show BIU spikes in the same locations. This will enable easier co-adding. (Caveat: the first one of a set will still be different, as explained in point 1).
3. Commanding all scans to a length of EVEN seconds poses a risk as well as the potential reward of easier co-adding. The risk is that for a short command length (e.g. 32 RTI), the interference may be seen only in the exact middle of the IFM. This may coincide with the area of ZPD, posing problems for interference-domain spike subtraction. In addition, the problem will be the same on every scan of the set. To prevent this, it may be wiser to set scan lengths to ODD numbers of seconds. This will cause the BIU interference to have a repeat of every 2, rather than every, scan. If however the BIU spike does occur in the ZPD region on some scans, it will be displaced by 8 RTI on the alternate scans. Hence, the spikes will always at least be easily spotted on alternate scans. On long scans (RTI >32) EVEN RTI values will not pose this problem, because the long positive path difference section will exhibit multiple BIU spikes, leading to easy determination of the offset S_0.

Appendices

A. BIU Interference Observed at ICO1

Figure 9 shows examples of FP1 IFMs and their magnitude spectra from the ICO1 (Instrument Check-Out 1) sequence. The IFMs are on the left and the resulting magnitude spectra are on the right.

In the inferferogram domain, note (a) the large spikes at regular intervals, and (b) the prominent sine wave ripple. The visible, regular spike pattern is just one of two such patterns, and occurs at the present time at intervals of 2 s (0.5 Hz), although the frequency was higher (0.75 Hz) during the ICO1 checkout and data displayed here. The second pattern is of lower amplitude and is buried in the noise here, but appears on large averages. Its frequency is 8 Hz (1/8 sec).

In the spectral domain, the 0.5 Hz and 8 Hz spikes are transformed into spike patterns at regular intervals. The 8 Hz peak is at 192 cm^{-1}, the 16 Hz overtone at 384 cm^{-1} and the 24 Hz at 576 cm^{-1}, on FP1. On FP3 the 32 Hz and 40 Hz overtones appear, however there is no visible effect on FP4. The sine wave is transformed to a large, low frequency spike near the origin on the spectra in these figures, although its frequency (and hence position on the spectra) is highly variable.

The frequency of 0.75 Hz implies that there are three queries every four seconds. However, these are not evenly spaced, and apparently can only happen when the RTI counter increments. This discretization effect causes the actual spikes to occur every (11, 11, 10) RTIs (1 RTI = 1/8 sec) for a total period of 32 RTIs or 4 seconds. In other words, rather than having the first three queries after 1.333, 2.667, 4.000 seconds; the actual queries happen on the nearest RTI, so 1.375, 2.750, 4.000 seconds.

On the actual interferogram, there are approximately 7.404 FP1 samples per RTI. This number is set by the mirror scan velocity. Hence, we expect the first three spikes to occur on samples 81.440, 162.888 and 236.928. However, the interferogram is itself discretised, so we actually see the interference on samples 81, 163 and 237, leading to a repeat period of 81, 82, 74 samples. Several caveats apply.

Firstly, depending on the scan mirror position relative to the RTI count, there will be an offset number S_0 samples, where S_0 is a positive or negative real number, for the location of the first spike. For example, the CDS cycle might be 16 RTIs (2 seconds) into its 4-second cycle, or 118.467 samples, when the first point of the interferogram is taken (The CDS and sampling cycles are unrelated, except that both must start and finish on a whole number of RTIs). Then, we would already have missed the first spike of the three-spike cycle, and would see the second one at sample (162.888-118.467) =44.421 =44. The second spike on the interferogram would be the third spike of the CDS cycle, at (236.928-118.467) =118.533 =119.

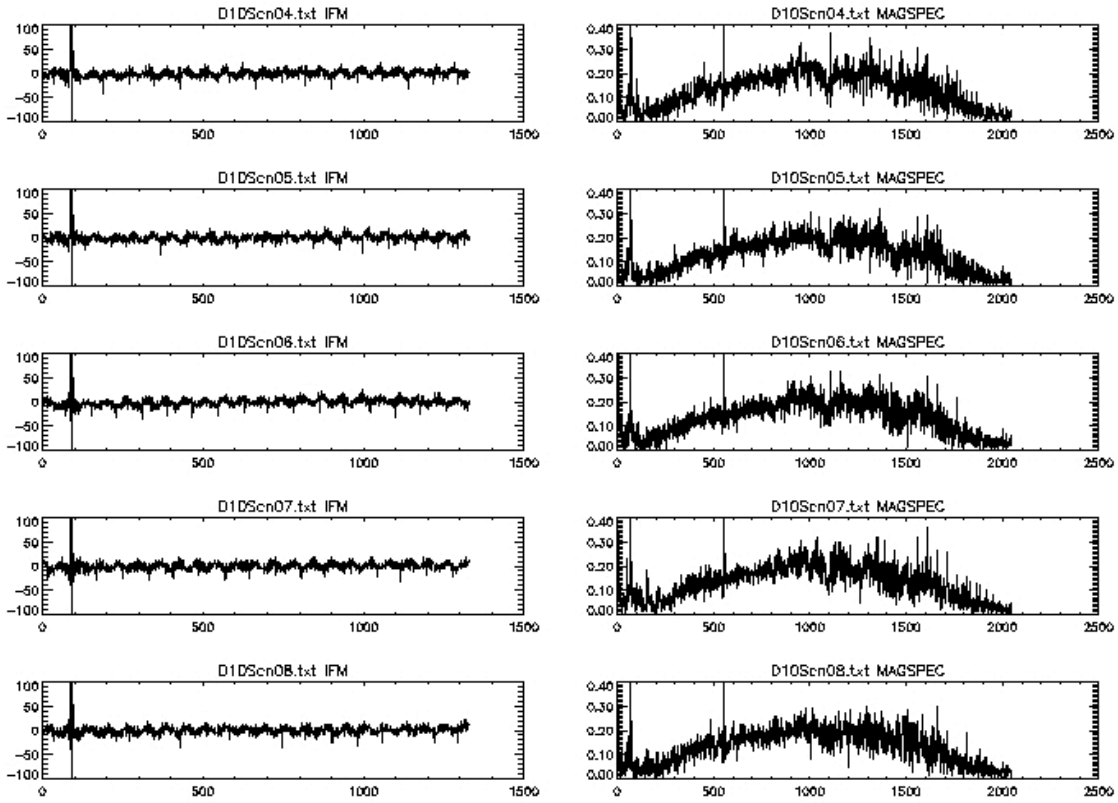

Figure 9: sequence of 200 RTI FP1 scans from ICO1 Day 10 (10 January, 1999; before cooler release).

A general set of formulae for the positions of the 0.75 Hz spikes on the ICO1 data is therefore:

$s_{(3n+0)} = \mathrm{NInt}(S_0 + (7.404 \times (11 + 32n)))$, $(n = 0,1,2,\ldots)$
$s_{(3n+1)} = \mathrm{NInt}(S_0 + (7.404 \times (22 + 32n)))$
$s_{(3n+2)} = \mathrm{NInt}(S_0 + (7.404 \times (32 + 32n)))$

where 'Nint' indicates the process of taking the nearest integer to the real value.

Secondly, we may not always see the repeat pattern (81, 82, 74) because of the interaction between the real period of 236.928 and the discretisation. For example, we may sometimes observe the period (81, 81, 74) or (81, 82, 73), because occasionally we have to drop a sample, to make the average period for the whole pattern equal to 236.928 rather than 237.

Thirdly, depending on the actual time taken for the CDS transfer to occur, the interference may spread over more than one sample. For example, if the CDS interrupt

happens at sample 81.440, both samples 81 and 82 may show interference. However, if the interrupt happened to occur at sample 80.999, only sample 81 may be affected.

We may now address the question of co-adding, or stacking interferograms. The key issue is whether the length of the scan in RTIs is a whole number of repeat periods or not. The repeat period of the interference is 32 RTIs. Hence, if a set of scans were taken which had a length of 32 RTIs[2] then on scan one we would see spikes at samples (81, 163, 237, …), and on scan two, we would also see spikes at (81, 163, 237, …) for the entire set of scans. Hence, a vertical plot of IFMs would always show the interference spikes lining up at the same sample points, and we could co-add IFMs easily.

Now consider the case where the scan length was 33 RTIs. At the end of the first scan, we would already be 1 RTI into the next cycle of interference. Hence the first spike on the second scan would occur not at RTI #11 (sample 81) but at RTI #10 (sample 74). The second spike on the second scan would be at RTI #21 rather than #22, etc. In this case, a vertical plot of IFMs would show a systematic drift in the absolute spike positions, even though the interval between them is unchanged. In fact, by the time we reach the 33rd IFM, the two cycles will be in step once again, and the spikes on IFM #33 will line up with the spikes on IFM #1.

In general therefore, we can predict exactly how many scans will occur before the interference is seen again at the same sample numbers in the IFM. We calculate the `left-over' number of RTIs R, which equals the scan length in RTIs modulo 32. We then find the lowest common multiple of the interference period (32) and the remainder R, and divide by R to find the repeat period in scans. For example, a scan of length 224 RTIs is exactly divided by 32, so the interference will repeat in the same place on every scan. A scan of length 404 RTIs however has 20 left-over RTIs at the end, and will take 8 scans for the pattern to repeat. A scan length of 200 RTIs has a remainder of 8, and will take 4 scans for the spikes to repeat (see Figure 10). The longest possible number of scans take for a repeat to occur is 32.

It is worth noting that, even allowing for this periodicity, the samples still may not occur in exactly the same place. For example, if the repeat pattern was 4 scans, and the first spike was at sample 81 on IFM #1, it may be at sample 82 on IFM #5, due to the vagaries of the discretization. In practice, when many scans are co-added, which nominally have the spikes in the same places, the spikes may spread over two samples on the final co-added IFM due to this ‘discretization jitter'.

---

[2] Interferogram scan length in RTIs includes not only the data-taking segment, but also the mirror flyback, and any other inactive time. It is measured from fly-back to fly-back (CIRS Flight Software Manual, Section 2.7.1). For example, a 200 RTI scan may only.have ~180 RTIs of data.

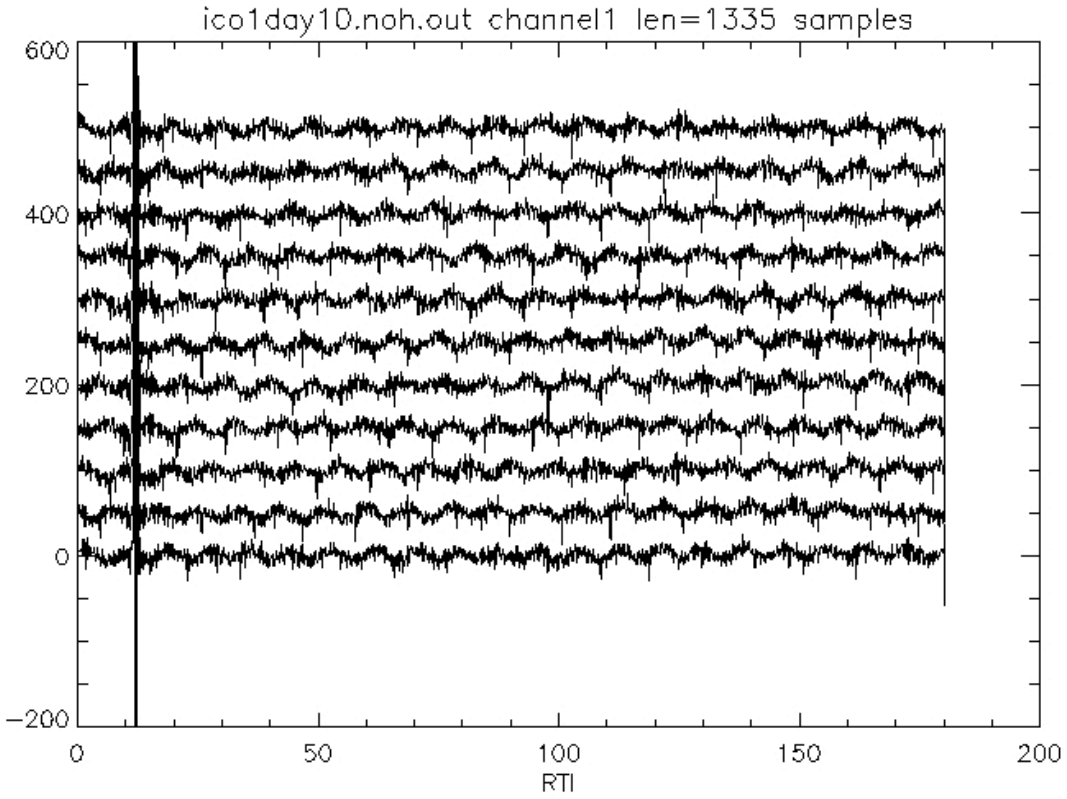

Figure 10: sequence of 200 RTI FP1 scans from ICO1 Day 10 (before cooler cover release). Note that the large interference spikes are repeated every fourth scan.

B. Calculation of time interval from start of 'scan' to ZPD

This section details the procedure for estimating the length of time t_{zpd} which elapses from the start of a 'scan' to the ZPD position.[3] This time period is comprised of two distinct mirror motions:

1. Flyback (t_{fb}).
2. Scanning at negative path difference (t_{nps}).

Therefore: $t_{zpd} = t_{fp} + t_{nps}$.

[3] The quotes around 'scan' indicate a *logical* scan, i.e. a scan command to the instrument. The 'scan' does not in fact begin with forward mirror motion (a *physical* scan) but flyback from the previous scan.

Times here are given in RTI (1/8 sec), the fundamental time unit of the instrument, but seconds could equally be used. Finally, to compute the clock time, e.g. SCET at ZPD, add the SCET at start of logical scan to t_{zpd} (in seconds).

B.1 Flyback motion

This is the time for the mirror to move back from the end of previous scan, to the start position for the next scan. This is a variable time, depending on how long (what resolution) the mirror traveled on the previous scan. However, it may be deduced by knowing two pieces of information.

1. The number of RTIs (=1/8 s) in the complete *current* scan plus flyback (t_{tot}, otherwise known as the *logical* scan). We do not need to know the length of the previous scan, because its flyback is included in the current scan. This number is set by commanding the instrument, and will also be output from the science packets into the OBS tables.
2. The time the mirror moved in actual foward scanning (t_{fmm}, otherwise known as the *physical* scan). The way to calculate this is to find the number of sample points in the interferogram n_s and then divide by the number of samples per RTIs, which is a fixed number for each focal plane derived from other constants (mirror travel speed and re-sampling factor) For example, s_{FP1}=7.404 samples per RTI (subject to small variations, due to mirror speed variations which we shall ignore).

Then: $t_{fp} = t_{tot} - t_{fmm}$.

B.2 Scanning at negative path difference

This is defined as the time for the mirror to reach the ZPD point from the kickoff position (at negative x). This time will be more or less constant, because the mirror always flies back to the same position, and travels forward to the ZPD at a near-constant speed. Like the flyback, this time is also the same for all focal planes. To calculate this time from an interferogram, firstly the ZPD must be found (sample which has the greatest absolute value will be close enough in most cases).

Then: $t_{nps} = n_{ZPD} / s$

B.3 Examples

<u>Example 1</u>

I took a ‘224 RTI' scan from ICO2. The number of FP1 samples in the IFM n_s=1510, corresponding to 1510/7.404 = 204 RTIs of actual data taking. The flyback time was then 20 RTIs.

The ZPD appeared at sample 90. Note that for FP1 the mean level of the IFM may not be zero, so you will need to subtract the mean level of the IFM away from ZPD from the

overall scan, before deciding where the max/min is. Or you could choose an IFM from fp3 or fp4 which are pretty close to zero mean level.

Hence, the negative path-difference part of the IFM took 90/7.404 = 12 RTI.

Finally, the time from start of `scan' i.e. scan time stamp to ZPD was actually 32 RTI = 4 secs.

Example 2

A ‘112' RTI scan. 705 points in IFM, ZPD at sample 90.

t_{fmm} = 95
t_{fb} = 112 - 95 = 17
t_{nps} = 12
t_{zpd} = 12+17 = 29 RTI = 3.6 s

C. Calibration Equations

C.1 Far-Infrared

In the far-infrared, the FP1 detector is at the same temperature as the instrument. Hence only a single calibration target (deep space) is required:

Equation 4: far-IR (FP1) calibration equation.

$$S_{t\,\mathrm{arg}} = \frac{FFT[I_{t\,\mathrm{arg}} - I_{space}]}{FFT[I_{space}]} \times [B(T_{instr})]$$

where *I* denotes an interferogram and, *S* denotes the Planck function, and *S* denotes a radiance spectrum.

C.2 Mid-Infrared

In the mid-infrared, two calibration targets are used due to the difference in temperature between the mid-IR FPA and the rest of the instrument:

Equation 5: mid-IR (FP3-FP4) calibration equation.

$$S_{t\,\mathrm{arg}} = \frac{FFT[I_{t\,\mathrm{arg}} - I_{space}]}{FFT[I_{shut} - I_{space}]} \times [B(T_{shut}) - B(T_{space})]$$